Forced vibration analysis of sandwich plates with an auxetic honeycomb core and laminated composite three-phase skin layers resting on Kerr foundation

Le Truong Son*

Faculty of Mechanical Engineering, Le Quy Don Technical University, 236 Hoang Quoc Viet, Bac Tu Liem, Hanoi, Vietnam.

*Corresponding author: letruongson01@gmail.com

Received 10 Dec. 2024; Revised 25 Feb. 2025; Accepted 09 May 2025; Published 25 May 2025.

DOI: https://doi.org/10.54939/1859-1043.j.mst.103.2025.110-120

ABSTRACT

This paper introduces isogeometric analysis (IGA) based on higher-order shear deformation theory (HSDT) for vibration analysis of sandwich plates resting on Kerr foundation (KF). The sandwich plates include the ultra-light of an auxetic honeycomb core layer and are reinforced by two laminated composite three-phase skin layers. The governing equation is derived from Hamilton's principle. The Newmark-β method is applied to solve the forced vibration of the sandwich plates by the code in Matlab software. The accuracy of the proposed method is verified through comparative examples. Additionally, the effects of geometrical dimensions, material properties, and foundation stiffness on the forced vibration of sandwich plates are studied in detail.

Keywords: Sandwich plates; Isogeometric analysis; Auxetic honeycomb; Kerr foundation; Forced vibration.

1. INTRODUCTION

Recent advances in additive manufacturing (AM) have revolutionized the design and production of complex bio-inspired engineering structures, of which negative Poisson's ratio honeycomb structures are no exception. Early studies on honeycomb structures yielding negative Poisson's ratio and its advantages were introduced by Wan et al. [1] and Zhang et al. [2]. Then, Zhu et al. [3] used the Galerkin solution to study the nonlinear vibration of honeycomb sandwich plates. Cong et al. [4] modified a third-order exact solution to analyze the dynamic behavior of sandwich shells. Duc et al. [5] showed the effects of geometrical parameters, and material properties on vibration of honeycomb sandwich plates by using an exact solution. Due to the use of analytical methods, the above studies are limited to complex models and arbitrary boundary conditions (BCs). Then, Tran et al. [6] examined the forced vibration of honeycomb sandwich plates based on first-order finite element formulation. Besides, several authors have introduced different methods in combination with different plate theories to examine the mechanical behavior of three-phase polymer/GNP/fiber structures including Cheng et al. [7], Swain et al. [8], Saeedi et al. [9], Yousefi et al. [10], Noroozi et al. [11]. The results from the above studies demonstrate the durability of the three-phase polymer/GNP/fiber structure and its perfect suitability as the skin of a sandwich structure.

Nowadays, with the development of computer technology, FEM and meshless methods can solve many engineering problems with different levels of complexity, however, for structures with complex geometry, the problem of meshing or dividing points can become a problem. To overcome this problem, the isogeometric method (IGA) has been a topic attracting much research in recent years. The isogeometric method is a numerical method proposed by Hughes et al. [12], which is a combination of Computer-Aided Design (CAD) geometric modeling and FE analysis. This combination is expressed in the use of the same shape functions in the geometric and finite element models, so instead of using basic shape functions based on Lagrange polynomials, IGA uses basic shape functions in the geometric model (B-splines). The IGA approach allows approximating field variables, instead of element nodes, on geometric key points, which reduces the computational load, especially the meshing difficulty for complex geometries.

It can be seen that IGA is a modern numerical method, most suitable for analyzing the mechanical behavior of structures. With that goal in mind, in this study, we introduce an IGA procedure based on Reddy's HSDT to analyze the forced vibrations of sandwich plates resting on KF. The accuracy and reliability of the proposed method are verified through comparative examples. In addition, the effect of geometrical dimensions and material properties on the forced vibration of sandwich plates is examined in detail.

For the convenience of readers, this paper is structured as follows: in addition to the introduction, the problem model is presented in section 2. Section 3 gives the basic equations. Numerical examples are performed in section 4. Finally, section 5 summarizes some of the main conclusions of the paper.

2. MODEL PROBLEM

2.1. The auxetic honeycomb core

Considering the sandwich plate with geometrical parameters as shown in figure 1. A group of $(h_1 - h_2 - h_3)$ denotes the sandwich plate's bottom-core-top skin layer thickness ratio.

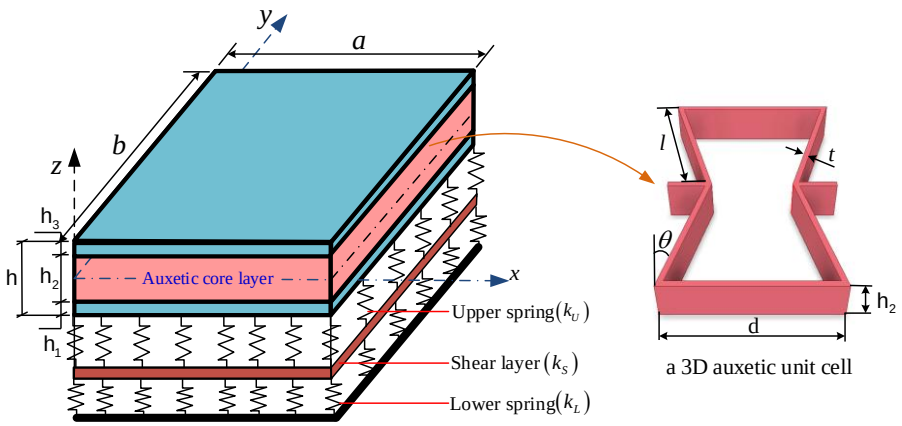

Figure 1. *The sandwich plate model resting on KF.*

The honeycomb core with mechanical properties is determined by [3]:

$$E_1^c = E_0 \frac{\lambda_3^3(\lambda_1 - sin\theta)}{cos\theta[cos^2\theta + \lambda_3^2(\lambda_1 + sin^2\theta)]};\ E_2^c = E_0 \frac{\lambda_3^3}{cos\theta(\lambda_1 - sin\theta)(tan^2\theta + \lambda_3^2)};$$

$$G_{12}^c = E_0 \frac{\lambda_3^3}{\lambda_1(1+2\lambda_1)cos\theta};\ G_{13}^c = G_0 \frac{\lambda_3}{2cos\theta}\left[\frac{\lambda_1 - sin\theta}{1+2\lambda_1} + \frac{\lambda_1 + 2sin^2\theta}{2(\lambda_1 - sin\theta)}\right];\ G_{23}^c = G_0 \frac{\lambda_3 cos\theta}{\lambda_1 - sin\theta}; \quad (1)$$

$$\rho^c = \rho_0 \frac{\lambda_3(\lambda_1+2)}{2cos\theta(\lambda_1 - sin\theta)};\ \upsilon_{12}^c = \frac{-sin\theta(\lambda_1 - sin\theta)(1-\lambda_3^2)}{[cos^2\theta + \lambda_3^2(\lambda_1 + sin^2\theta)]};\ \upsilon_{21}^c = \frac{-sin\theta(1-\lambda_3^2)}{(tan^2\theta + \lambda_3^2)(\lambda_1 - sin\theta)}.$$

where $\lambda_1 = d/l$ and $\lambda_3 = t/l$ with l is the length of the inclined cell rib, d is the length of the vertical cell rib, t is the thickness of honeycomb unit cell rib, and θ is the inclined angle as shown in figure 1.

2.2. The three-phase skin layer

2.2.1. The GNP-reinforced polymer

According to the rule of mixture, the Poisson's ratio υ_{Gm} and the density ρ_{Gm} of the GNP are gained ($V_m + V_{GNP} = 1$) as follows:

$$\upsilon_{Gm} = \upsilon_m V_m + \upsilon_{GNP} V_{GNP};\ \rho_{Gm} = \rho_m V_m + \rho_{GNP} V_{GNP} \quad (2)$$

The GNP volume fraction is calculated through the weight fraction (W_{GNP}) as follows [13]:

$$V_{GNP} = \frac{\rho_m W_{GNP}}{\rho_m + \rho_{GNP}(1 - W_{GNP})} \tag{3}$$

The GNP-reinforced polymer's elastic modulus is obtained using the Halpin-Tsai model [14]:

$$E_{Gm} = \left(\frac{5}{8}\frac{1 + \xi_W \eta_W V_{GNP}}{1 - \eta_W V_{GNP}} + \frac{3}{8}\frac{1 + \xi_L \eta_L V_{GNP}}{1 - \eta_L V_{GNP}}\right) E_m \tag{4a}$$

in which

$$\xi_W = \frac{2W_{GNP}}{h_{GNP}};\ \xi_L = \frac{2l_{GNP}}{h_{GNP}};\ \eta_W = \frac{\eta - 1}{\eta + \xi_W};\ \eta_L = \frac{\eta - 1}{\eta + \xi_L};\ \eta = \frac{E_{GNP}}{E_m};\ G_{Gm} = \frac{E_{Gm}}{2(1 + \upsilon_{Gm})} \tag{4b}$$

with $W_{GNP}, l_{GNP}, and\ h_{GNP}$ denote the width, length, and thickness of the GNPs, respectively.

2.2.2. The three-phase skin layers

A three-phase polymer/GNP/fiber density is defined according to the rule of the mixture as follows ($V_{Gm} + V_F = 1$):

$$\rho_f = \rho_F V_F + \rho_{Gm} V_{Gm} \tag{5}$$

with the fibers volume fraction is defined following weight fraction (W_F) by:

$$V_F = \frac{\rho_{Gm} W_F}{\rho_{Gm} + \rho_F (1 - W_F)} \tag{6}$$

For the three-phase skin layers, the elastic moduli (E_{ij}^f), shear moduli (G_{ij}^f), and Poisson's ratio (υ_{ij}^f) as obtained as follows [6]:

$$\begin{gathered}
E_{11}^f = E_{11}^F V_F + E_{Gm} V_{Gm};\ E_{22}^f = \left(\frac{E_{22}^F + E_{Gm} + (E_{22}^F - E_{Gm})V_F}{E_{22}^F + E_{Gm} - (E_{22}^F - E_{Gm})V_F}\right) E_{Gm};\\
G_{12}^f = G_{13}^f = \left(\frac{G_{22}^F + G_{Gm} + (G_{22}^F - G_{Gm})V_F}{G_{22}^F + G_{Gm} - (G_{22}^F - G_{Gm})V_F}\right) G_{Gm};\ G_{23}^f = \frac{E_{22}^f}{2\left(1 + \upsilon_{23}^f\right)};\\
\upsilon_{12}^f = \upsilon_{12}^F V_F + \upsilon_{Gm} V_{Gm};\ \upsilon_{21}^f = \frac{E_{22}^f}{E_{11}^f}\upsilon_{12}^f;\\
\upsilon_{23}^f = \upsilon_{12}^F V_F + \upsilon_{Gm} V_{Gm}\left(\frac{1 + \upsilon_{Gm} + \upsilon_{12}^f \frac{E_{Gm}}{E_{11}^f}}{1 + \upsilon_{Gm}^2 + \upsilon_{12}^f \upsilon_{Gm} \frac{E_{Gm}}{E_{11}^f}}\right)
\end{gathered} \tag{7}$$

herein, symbols GNP, m, Gm, f and F represent the GNPs, polymeric matrix, GNP-reinforced matrix, skin layers, and fibers, respectively.

2.3. Kerr foundation

KF consists of an upper layer k_U, a shear layer k_S and a lower layer k_L are defined by [15]:

$$\boldsymbol{\mathcal{R}} = \frac{k_L k_U}{k_L + k_U} w(x,y) - \frac{k_S k_U}{k_S + k_U}\left(\left(\frac{\partial w}{\partial x}\right)^2 + \left(\frac{\partial w}{\partial y}\right)^2\right) \tag{8}$$

The KF becomes to Pasternak foundation (PF) when k_U gets infinity:

$$\boldsymbol{\mathcal{R}} = k_L w(x,y) - k_S\left(\left(\frac{\partial w}{\partial x}\right)^2 + \left(\frac{\partial w}{\partial y}\right)^2\right) \tag{9}$$

2.4. Pulse loads

This paper uses the types of pulse, including step load, triangular load, and blast load as follows:

- Step loading:

$$p(t) = \begin{cases} P_0 & 0 \le t \le t_s \\ 0 & t \ge t_s \end{cases} \tag{10a}$$

- Triangular loading:

$$p(t) = \begin{cases} P_0\left(1 - \dfrac{t}{t_s}\right) & 0 \le t \le t_s \\ 0 & t \ge t_s \end{cases} \tag{10b}$$

- Blast loading:

$$p(t) = p(t) = \begin{cases} P_0\left(1 - \dfrac{t}{t_s}\right)e^{-\gamma t/t_s} & 0 \le t \le t_s \\ 0 & t \ge t_s \end{cases} \tag{10c}$$

in which P_0 represents the peak value of different pulse loads, t_s denotes the duration of the load, and γ is the attenuation coefficient of blast load.

3. BASIS FORMULATION

3.1. The displacement field

Following Reddy's HSDT, the displacement field is determined by [16]:

$$\begin{cases} u(x,y,z) = u_0(x,y) - z\theta_x + cz^3\left(\theta_x + w_{,x}\right) \\ v(x,y,z) = v_0(x,y) - z\theta_y + cz^3\left(\theta_y + w_{,y}\right) \\ w(x,y,z) = w(x,y). \end{cases} \tag{11}$$

where $c = -\frac{4}{3h^2}$ and u_0, v_0, θ_x, θ_y, and w are unknown variables. To ensure the continuity of the deformation field and to be able to apply the HSDT. It is assumed that the layers do not separate from each other during deformation.

The strain-displacement relation is defined by

$$\boldsymbol{\varepsilon} = \boldsymbol{\varepsilon_m} + z\boldsymbol{\kappa}_1 + z^3\boldsymbol{\kappa}_2; \boldsymbol{\gamma} = \boldsymbol{\varepsilon}_s + z^2\boldsymbol{\kappa}_s \tag{12}$$

in which

$$\boldsymbol{\varepsilon_m} = \begin{Bmatrix} u_{0,x} \\ v_{0,y} \\ u_{0,y} + v_{0,x} \end{Bmatrix}; \boldsymbol{\kappa}_1 = \begin{Bmatrix} \theta_{x,x} \\ \theta_{x,y} \\ \theta_{x,y} + \theta_{y,x} \end{Bmatrix}; \boldsymbol{\kappa}_2 = c\begin{Bmatrix} \theta_{x,x} + w_{,xx} \\ \theta_{y,y} + w_{,yy} \\ \theta_{x,y} + \theta_{y,x} + 2w_{,xy} \end{Bmatrix}; \tag{13a}$$

$$\boldsymbol{\varepsilon}_s = \begin{Bmatrix} \theta_x + w_{,x} \\ \theta_y + w_{,y} \end{Bmatrix}; \boldsymbol{\kappa}_s = 3c\begin{Bmatrix} \theta_x + w_{,x} \\ \theta_y + w_{,y} \end{Bmatrix} \tag{13b}$$

Note that the symbols $_{,x}$ and $_{,y}$ are the first derivatives of the displacement components with respect to x and y; $_{,xx}$, $_{,yy}$, and $_{,xy}$ are the second derivatives of the displacement components with respect to x and y, respectively.

The stress-strain relation according to Hooke's law is obtained as follows:

$$\begin{Bmatrix} \sigma_x \\ \sigma_y \\ \tau_{xy} \\ \tau_{xz} \\ \tau_{yz} \end{Bmatrix} = \begin{bmatrix} Q_{11} & Q_{12} & 0 & 0 & 0 \\ Q_{21} & Q_{22} & 0 & 0 & 0 \\ 0 & 0 & Q_{66} & 0 & 0 \\ 0 & 0 & 0 & Q_{55} & Q_{45} \\ 0 & 0 & 0 & Q_{45} & Q_{44} \end{bmatrix} \begin{Bmatrix} \varepsilon_x \\ \varepsilon_y \\ \gamma_{xy} \\ \gamma_{xz} \\ \gamma_{yz} \end{Bmatrix} \tag{14}$$

where

For the auxetic honeycomb core [16]:

$$Q_{11}^c = \frac{E_1^c}{1-\upsilon_{12}^c\upsilon_{21}^c}; Q_{22}^c = \frac{E_2^c}{1-\upsilon_{12}^c\upsilon_{21}^c}; Q_{12}^c = Q_{21}^c\frac{\upsilon_{12}^c E_1^c}{1-\upsilon_{12}^c\upsilon_{21}^c}$$
$$Q_{44}^c = G_{23}^c; Q_{55}^c = G_{13}^c; Q_{66}^c = G_{12}^c; Q_{45}^c = 0. \tag{15}$$

For the three-phase skin layers [16]:

$$\begin{bmatrix} Q_{11}^s & Q_{12}^s & Q_{16}^s & 0 & 0 \\ Q_{12}^s & Q_{22}^s & Q_{26}^s & 0 & 0 \\ Q_{16}^s & Q_{26}^s & Q_{66}^s & 0 & 0 \\ 0 & 0 & 0 & Q_{55}^s & Q_{45}^s \\ 0 & 0 & 0 & Q_{45}^s & Q_{44}^s \end{bmatrix} = \tag{16}$$

$$\begin{bmatrix} m^2 & n^2 & -2mn & 0 & 0 \\ n^2 & m^2 & 2mn & 0 & 0 \\ mn & -mn & m^2-n^2 & 0 & 0 \\ 0 & 0 & 0 & m & -n \\ 0 & 0 & 0 & n & m \end{bmatrix} \begin{bmatrix} \bar{Q}_{11}^s & \bar{Q}_{12}^s & 0 & 0 & 0 \\ \bar{Q}_{12}^s & \bar{Q}_{22}^s & 0 & 0 & 0 \\ 0 & 0 & \bar{Q}_{66}^s & 0 & 0 \\ 0 & 0 & 0 & \bar{Q}_{55}^s & 0 \\ 0 & 0 & 0 & 0 & \bar{Q}_{44}^s \end{bmatrix} \begin{bmatrix} m^2 & n^2 & -2mn & 0 & 0 \\ n^2 & m^2 & 2mn & 0 & 0 \\ mn & -mn & m^2-n^2 & 0 & 0 \\ 0 & 0 & 0 & m & -n \\ 0 & 0 & 0 & n & m \end{bmatrix}^T$$

where $m = \cos(\varphi_k)$ and $n = \sin(\varphi_k)$ in which φ_k stands for the fiber angle in the k^{th} layer, and

$$\bar{Q}_{11}^s = \frac{E_{11}^f}{1-\upsilon_{12}^f \upsilon_{21}^f}; \bar{Q}_{22}^s = \frac{E_{22}^f}{1-\upsilon_{12}^f \upsilon_{21}^f}; \bar{Q}_{12}^s = \upsilon_{12}^f \bar{Q}_{22}^s; \\ \bar{Q}_{44}^s = G_{23}^f; \bar{Q}_{55}^s = G_{13}^f; \bar{Q}_{66}^s = G_{12}^f. \tag{17}$$

The stress resultants are computed by:

$$\begin{Bmatrix} \mathbb{N} \\ \mathcal{M} \\ \wp \end{Bmatrix} = \mathbb{C}_1 \begin{Bmatrix} \boldsymbol{\varepsilon_m} \\ \boldsymbol{\kappa}_1 \\ \boldsymbol{\kappa}_2 \end{Bmatrix}; \begin{Bmatrix} \mathbb{Q} \\ \mathbb{R} \end{Bmatrix} = \mathbb{C}_2 \begin{Bmatrix} \boldsymbol{\varepsilon}_s \\ \boldsymbol{\kappa}_s \end{Bmatrix} \tag{18}$$

where

$$\mathbb{C}_1 = \begin{bmatrix} \mathbb{A} & \mathbb{B} & \mathbb{B}^b \\ \mathbb{B} & \mathbb{F} & \mathbb{F}^b \\ \mathbb{B}^b & \mathbb{F}^b & \mathbb{H} \end{bmatrix}; \mathbb{C}_2 = \begin{bmatrix} \mathbb{A}^s & \mathbb{B}^s \\ \mathbb{B}^s & \mathbb{F}^s \end{bmatrix} \tag{19}$$

with $\mathbb{A}, \mathbb{B}, \mathbb{F}, \mathbb{B}^b, \mathbb{F}^b, \mathbb{H}, \mathbb{A}^s, \mathbb{B}^s$ and $\mathbb{F}^s$ are the material matrices determined by:

$$\left(\mathbb{A}, \mathbb{B}, \mathbb{F}, \mathbb{B}^b, \mathbb{F}^b, \mathbb{H}\right) = \int_{\frac{-h}{2}}^{\frac{h}{2}} \begin{bmatrix} Q_{11} & Q_{12} & 0 \\ Q_{21} & Q_{22} & 0 \\ 0 & 0 & Q_{66} \end{bmatrix} (1, z, z^2, z^3, z^4, z^6) dz; \tag{20a}$$

$$(\mathbb{A}^s, \mathbb{B}^s, \mathbb{F}^s) = \int_{-h/2}^{h/2} (1, z^2, z^4) \begin{bmatrix} Q_{55} & Q_{45} \\ Q_{45} & Q_{44} \end{bmatrix} dz \tag{20b}$$

Replacing equation (19) into equation (18), we get:

$$\begin{Bmatrix} \mathbb{N} \\ \mathcal{M} \\ \wp \\ \mathbb{Q} \\ \mathbb{R} \end{Bmatrix} = \begin{bmatrix} \mathbb{A} & \mathbb{B} & \mathbb{B}^b & \mathbf{0} & \mathbf{0} \\ \mathbb{B} & \mathbb{F} & \mathbb{F}^b & \mathbf{0} & \mathbf{0} \\ \mathbb{B}^b & \mathbb{F}^b & \mathbb{H} & \mathbf{0} & \mathbf{0} \\ \mathbf{0} & \mathbf{0} & \mathbf{0} & \mathbb{A}^s & \mathbb{B}^s \\ \mathbf{0} & \mathbf{0} & \mathbf{0} & \mathbb{B}^s & \mathbb{F}^s \end{bmatrix} \begin{Bmatrix} \boldsymbol{\varepsilon_m} \\ \boldsymbol{\kappa}_1 \\ \boldsymbol{\kappa}_2 \\ \boldsymbol{\varepsilon}_s \\ \boldsymbol{\kappa}_s \end{Bmatrix} \tag{21}$$

3.2. The governing equations

The governing equation of the plate following Hamilton's principle is determined by [16]:

$$\int_0^T \left(\delta U + \delta U^f + \delta W - \delta T\right) dt = 0 \tag{22}$$

in which the virtual strain energy is determined by:

$$\delta U = \int_\Omega \left(\left(\delta \boldsymbol{\varepsilon}_m\right)^T \mathbb{N} + (\delta \boldsymbol{\kappa}_1)^T \mathcal{M} + (\delta \boldsymbol{\kappa}_2)^T \wp + (\delta \boldsymbol{\varepsilon}_s)^T \mathbb{Q} + (\delta \boldsymbol{\kappa}_s)^T \mathbb{R} \right) d\Omega. \tag{23}$$

The virtual work done by external forces as:

$$\delta W = -\int_\Omega q(t) \delta w \, d\Omega. \tag{24}$$

The virtual deformed foundation is defined by:

$$\delta U^f = \int_\Omega \boldsymbol{\mathcal{R}} \delta w \, \mathrm{d}\Omega \tag{25}$$

The virtual kinetic energy can be expressed by:

$$\delta T = \int_\Omega (\delta \dot{\boldsymbol{u}}_1^T \boldsymbol{\chi} \dot{\boldsymbol{u}}_1 + \delta \dot{\boldsymbol{u}}_2^T \boldsymbol{\chi} \dot{\boldsymbol{u}}_2 + \delta \dot{\boldsymbol{u}}_3^T \boldsymbol{\chi} \dot{\boldsymbol{u}}_3)\, dxdy = \int_\Omega \delta \dot{\boldsymbol{u}}^T \boldsymbol{\Upsilon} \dot{\boldsymbol{u}}\, d\Omega. \tag{26}$$

with $\boldsymbol{\Upsilon}$ is the matrix of inertial components:

$$\boldsymbol{\Upsilon} = \begin{bmatrix} \boldsymbol{\chi} & 0 & 0 \\ 0 & \boldsymbol{\chi} & 0 \\ 0 & 0 & \boldsymbol{\chi} \end{bmatrix} \text{ with } \boldsymbol{\chi} = \begin{bmatrix} l_0 & l_1 & l_3 \\ l_1 & l_2 & l_4 \\ l_3 & l_4 & l_6 \end{bmatrix}; \tag{27}$$

in there

$$(l_0, l_1, l_2, l_3, l_4, l_6) = \int_{-h/2}^{h/2} \rho(1, z, z^2, z^3, z^4, z^6) dz \tag{28}$$

where ρ is the mass density and displacement vectors are expressed by:

$$\begin{gathered} \boldsymbol{u} = \begin{Bmatrix} \boldsymbol{u}_1 \\ \boldsymbol{u}_2 \\ \boldsymbol{u}_3 \end{Bmatrix};\ \boldsymbol{u}_1 = \begin{Bmatrix} u_0 \\ -w_{,x} \\ \theta_x \end{Bmatrix};\ \boldsymbol{u}_2 = \begin{Bmatrix} v_0 \\ -w_{,y} \\ \theta_y \end{Bmatrix};\ \boldsymbol{u}_3 = \begin{Bmatrix} w \\ 0 \\ 0 \end{Bmatrix}; \\ \dot{\boldsymbol{u}}_1 = \begin{Bmatrix} \dot{u}_0 \\ -\dot{w}_{,x} \\ \dot{\theta}_x \end{Bmatrix};\ \dot{\boldsymbol{u}}_2 = \begin{Bmatrix} \dot{v}_0 \\ -\dot{w}_{,y} \\ \dot{\theta}_y \end{Bmatrix};\ \dot{\boldsymbol{u}}_3 = \begin{Bmatrix} \dot{w} \\ 0 \\ 0 \end{Bmatrix}. \end{gathered} \tag{29}$$

The weak form of the plate is determined by [16]:

$$\begin{gathered} \int_\Omega ((\delta \boldsymbol{\varepsilon})^T \mathbb{C}_1 \boldsymbol{\varepsilon} + (\delta \boldsymbol{\gamma})^T \mathbb{C}_2 \boldsymbol{\gamma})\, d\Omega + \int_\Omega \boldsymbol{\mathcal{R}}(\delta w)\, d\Omega + \int_\Omega \delta \boldsymbol{u}^T \boldsymbol{\Upsilon} \ddot{\boldsymbol{u}}\, d\Omega \\ = \int_\Omega q(t)(\delta w)\, d\Omega \end{gathered} \tag{30}$$

3.3. Isogeometric analysis procedure

The displacement field is approximated by the NURBS functions by [12]:

$$\boldsymbol{u}(\xi, \eta) = \sum_{K=1}^{p \times q} \boldsymbol{R}_K(\xi, \eta) \boldsymbol{d}_K \tag{31}$$

where $\boldsymbol{d}_K = \{u_{0K}, v_{0K}, w_K, \theta_{xK}, \theta_{yK}\}^T$ represents the displacement of control point K, and $\boldsymbol{R}_K$ denotes the shape function.

Substituting equation (31) into equation (13), we get:

$$[\boldsymbol{\varepsilon}_m;\ \boldsymbol{\kappa}_1;\ \boldsymbol{\kappa}_2;\ \boldsymbol{\varepsilon}_s;\ \boldsymbol{\kappa}_s] = \sum_{K=1}^{p \times q} [\boldsymbol{B}_m;\ \boldsymbol{B}_1;\ \boldsymbol{B}_2;\ \boldsymbol{B}_{s1};\ \boldsymbol{B}_{s2}] \boldsymbol{d}_K \tag{32}$$

in which

$$\boldsymbol{B}_m = \begin{bmatrix} \boldsymbol{R}_{K,x} & 0 & 0 & 0 & 0 \\ 0 & \boldsymbol{R}_{K,y} & 0 & 0 & 0 \\ \boldsymbol{R}_{K,y} & \boldsymbol{R}_{K,x} & 0 & 0 & 0 \end{bmatrix} \tag{33a}$$

$$\boldsymbol{B}_1 = \begin{bmatrix} 0 & 0 & 0 & \boldsymbol{R}_{K,x} & 0 \\ 0 & 0 & 0 & 0 & \boldsymbol{R}_{K,y} \\ 0 & 0 & 0 & \boldsymbol{R}_{K,y} & \boldsymbol{R}_{K,x} \end{bmatrix} \tag{33b}$$

$$\boldsymbol{B}_2 = c\begin{bmatrix} 0 & 0 & \boldsymbol{R}_{K,xx} & \boldsymbol{R}_{K,x} & 0 \\ 0 & 0 & \boldsymbol{R}_{K,yy} & 0 & \boldsymbol{R}_{K,y} \\ 0 & 0 & 2\boldsymbol{R}_{K,xy} & \boldsymbol{R}_{K,y} & \boldsymbol{R}_{K,x} \end{bmatrix} \tag{33c}$$

$$\boldsymbol{B}_{s1} = \begin{bmatrix} 0 & 0 & \boldsymbol{R}_{K,x} & \boldsymbol{R}_K & 0 \\ 0 & 0 & \boldsymbol{R}_{K,y} & 0 & \boldsymbol{R}_K \end{bmatrix}; \boldsymbol{B}_{s2} = 3c\begin{bmatrix} 0 & 0 & \boldsymbol{R}_{K,x} & \boldsymbol{R}_K & 0 \\ 0 & 0 & \boldsymbol{R}_{K,y} & 0 & \boldsymbol{R}_K \end{bmatrix} \tag{33d}$$

Substituting equation (32) into equation (30), the motion equation of plates is determined by

$$\boldsymbol{M}\ddot{\boldsymbol{q}} + \boldsymbol{C}\dot{\boldsymbol{q}} + \left(\boldsymbol{K} + \boldsymbol{K}^f\right)\boldsymbol{q} = \boldsymbol{F} \tag{34}$$

where the plate stiffness matrix is determined by:

$$\boldsymbol{K} = \int_\Omega \left(\begin{bmatrix} \boldsymbol{B}_m \\ \boldsymbol{B}_1 \\ \boldsymbol{B}_2 \end{bmatrix}^T \begin{bmatrix} \mathbb{A} & \mathbb{B} & \mathbb{B}^b \\ \mathbb{B} & \mathbb{F} & \mathbb{F}^b \\ \mathbb{B}^b & \mathbb{F}^b & \mathbb{H} \end{bmatrix} \begin{bmatrix} \boldsymbol{B}_m \\ \boldsymbol{B}_1 \\ \boldsymbol{B}_2 \end{bmatrix} + \begin{bmatrix} \boldsymbol{B}_{s1} \\ \boldsymbol{B}_{s2} \end{bmatrix}^T \begin{bmatrix} \mathbb{A}^s & \mathbb{B}^s \\ \mathbb{B}^s & \mathbb{F}^s \end{bmatrix} \begin{bmatrix} \boldsymbol{B}_{s1} \\ \boldsymbol{B}_{s2} \end{bmatrix} \right) d\Omega \tag{35}$$

The plate mass matrix defined by:

$$\boldsymbol{M} = \int_\Omega \begin{bmatrix} \boldsymbol{H}_1 \\ \boldsymbol{H}_2 \\ \boldsymbol{H}_3 \end{bmatrix}^T \begin{bmatrix} \boldsymbol{\chi} & 0 & 0 \\ 0 & \boldsymbol{\chi} & 0 \\ 0 & 0 & \boldsymbol{\chi} \end{bmatrix} \begin{bmatrix} \boldsymbol{H}_1 \\ \boldsymbol{H}_2 \\ \boldsymbol{H}_3 \end{bmatrix} d\Omega \tag{36}$$

with

$$\boldsymbol{H}_1 = \begin{bmatrix} \boldsymbol{R}_K & 0 & 0 & 0 & 0 \\ 0 & 0 & \boldsymbol{R}_{K,x} & 0 & 0 \\ 0 & 0 & 0 & \boldsymbol{R}_K & 0 \end{bmatrix}; \boldsymbol{H}_2 = \begin{bmatrix} 0 & \boldsymbol{R}_K & 0 & 0 & 0 \\ 0 & 0 & \boldsymbol{R}_{K,y} & 0 & 0 \\ 0 & 0 & 0 & 0 & \boldsymbol{R}_K \end{bmatrix}; \boldsymbol{H}_3 = \begin{bmatrix} 0 & 0 & \boldsymbol{R}_K & 0 & 0 \\ 0 & 0 & 0 & 0 & 0 \\ 0 & 0 & 0 & 0 & 0 \end{bmatrix} \tag{37}$$

The foundation stiffness matrix $\boldsymbol{K}^f$ is obtained by:

$$\begin{aligned} \boldsymbol{K}^f = \frac{k_L k_U}{k_L + k_U} \int_\Omega & (\boldsymbol{R}_K)^{\mathrm{T}} (\boldsymbol{R}_K) \mathrm{d}\Omega \\ & + \frac{k_S k_U}{k_S + k_U} \int_\Omega \left[\left(\boldsymbol{R}_{K,x}\right)^{\mathrm{T}} \left(\boldsymbol{R}_{K,x}\right) + \left(\boldsymbol{R}_{K,y}\right)^{\mathrm{T}} \left(\boldsymbol{R}_{K,y}\right) \right] \mathrm{d}\Omega \end{aligned} \tag{38}$$

The transverse load vector is gained as follows:

$$\boldsymbol{F} = \int_\Omega q(t)\boldsymbol{R}\, d\Omega \tag{39}$$

And, the damping matrix $\boldsymbol{C} = \alpha\boldsymbol{M} + \beta\boldsymbol{K}$, with α and β are Rayleigh damping factors defined through damping ratio ζ and the first two natural frequencies [17].

$$\beta = \frac{2\zeta}{\omega_1 + \omega_2};\ \alpha = \frac{2\omega_1\omega_2\zeta}{\omega_1 + \omega_2} \tag{40}$$

To solve equation (34), the Newmark-β method is used with steps as shown in [17].

4. NUMERICAL RESULTS

In this section, the constituent material properties are shown in table 1.

Table 1. *The adopted material properties [14].*

Materials	Young's modulus E (GPa)	Density ρ (kg/m^3)	Poisson's ratio υ
Al	70	2707	0.3
Al_2O_3	380	3800	0.3
Epoxy	3	1200	0.34
GNPs	1010	1060	0.186

4.1. Verification

Considering the fully simply supported (SSSS) functionally graded (FG) (Al/Al_2O_3) square plate with geometrical parameters $a = b = 0.2m,\ h = 0.025m$ under a step load $q_0(x, y) = 50MPa$. It can be seen that the gained deflection response is a good similarity both in shape and value with those of Abuteir et al. [18] using a degenerated shell element as shown in figure 2. This example has verified the accuracy of the proposed formula.

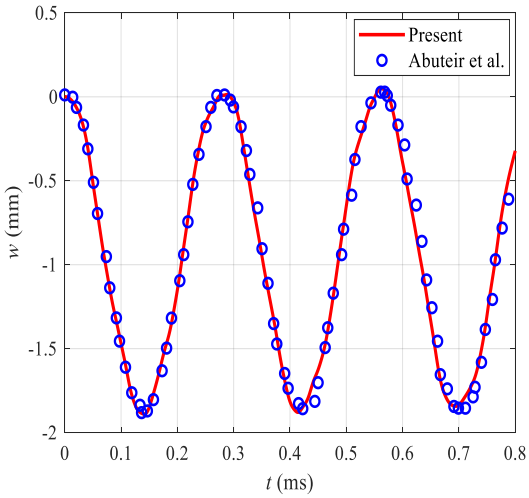

Figure 2. *The deflection response of SSSS FG square plate center.*

4.2. Dynamic response analysis

This section studies the sandwich plate with an auxetic honeycomb core and laminated three-phase polymer/GNP/fiber skin layers. The remaining structural parameters include the dimensions of the GNPs: $l_{GNP} = 2.5\mu m,\ w_{GNP} = 1.5\mu m,\ h_{GNP} = 1.5nm$ with weight fraction of the GNPs: $W_{GNP} = 0.01$; each face sheet consists of four layers of $\varphi = [90/45^0/45^0/90^0]$ with the glass fibers' mechanical properties: $E_{11}^F = E_{22}^F = 73.084GPa,\ G_{12}^F = 30.13GPa,\ \upsilon_{12}^F = 0.22,\ \rho_F = 2491.191Kg/m^3$, and $W_F = 0.85$; the auxetic honeycomb core is made of aluminium (Al).

Firstly, the effect of λ_1 on the forced vibration of SSSS square sandwich plates with layer thickness ratio (1-8-1) subjected to step load is presented in figure 3. The input parameters as $a/h = 50,\ \theta = 50^0,\ \lambda_3 = 0.15,\ K_L = K_U = 50$, and $K_S = 15$. Observing that λ_1 has no sensitive effect on the forced vibration of the plate. However, increasing λ_1 rapidly reduces plate oscillation.

Secondly, the impact of θ on the forced vibration of simply supported-clamped-simply supported-clamped (SCSC) square sandwich plates with layer thickness ratio (1-6-1) subjected to triangular load is presented in figure 4. The remaining parameters as $a/h = 60,\ \lambda_1 = 2,\ \lambda_3 = 0.1,\ K_L = K_U = 75$, and $K_S = 25$. It can be seen that the change of θ has little effect on the maximum displacement response of the sandwich plate but affects the speed of oscillation reduction of the sandwich plate. This is because the θ affects the Poisson's ratio, a negative Poisson's ratio increases the vibration absorption capacity, as expected.

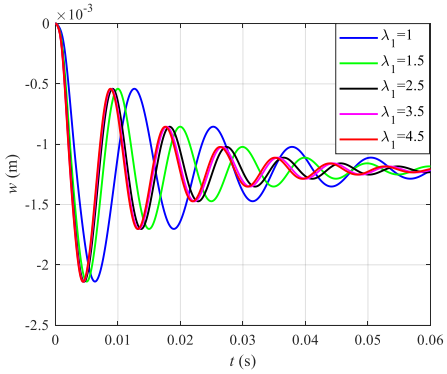

a) The centre deflection response;

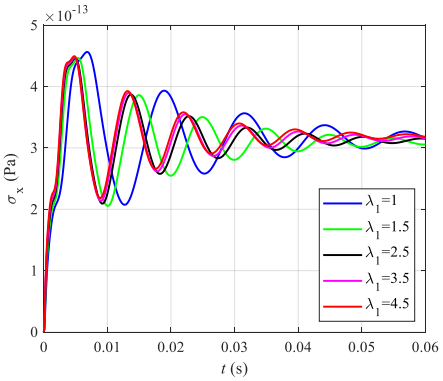

b) Stress response $\sigma_x(\frac{a}{2},\frac{b}{2},0)$.

Figure 3. *Effects of* λ_1 *on the forced vibration of SSSS sandwich plates under step load.*

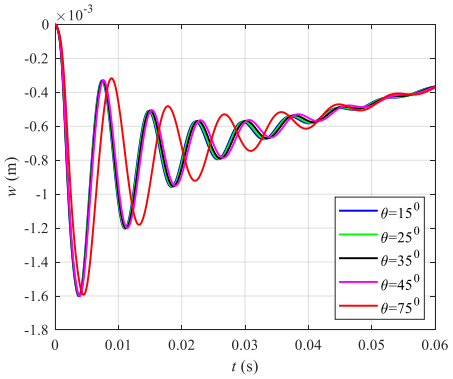

a) The centre deflection response;

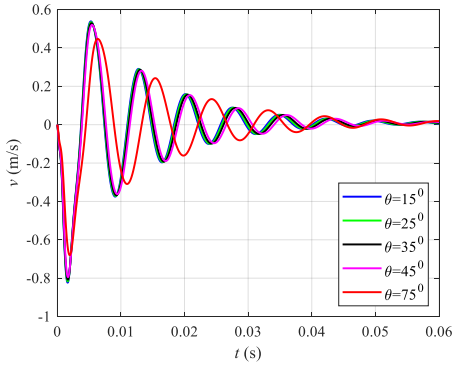

b) The centre velocity response.

Figure 4. *Effects of* θ *on the forced vibration of SCSC sandwich plates under triangular load.*

Finally, the effect of layer thickness ratio on the forced vibration of (fully clamped) CCCC square sandwich plates subjected to blast load is indicated in figure 5. The input parameters are $a/h = 75$, $\theta = 60^0$, $\lambda_1 = 4$, $\lambda_3 = 0.2$, $\gamma = 2$, $K_L = K_U = 75$, and $K_S = 45$. It can be found that the thicker the honeycomb core, the larger the displacement and stress response of the sandwich plate. Note that, the damping ratio $\zeta = 0.1$ for the above examines.

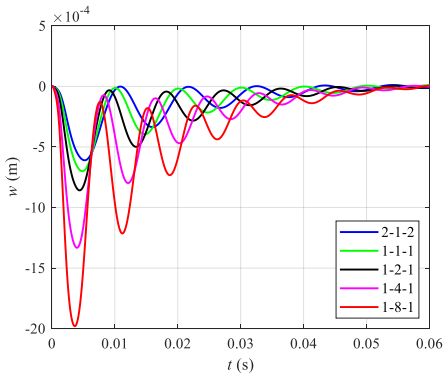

a) The deflection response;

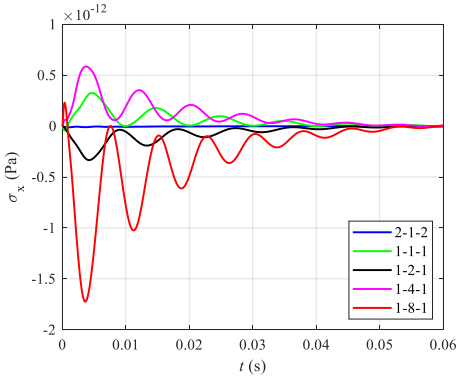

b) Stress response $\sigma_x(\frac{a}{2},\frac{b}{2},0)$.

Figure 5. *Effects of the thickness ratio on the forced vibration of CCCC sandwich plates under blast loading.*

5. CONCLUSIONS

In this article, the authors have successfully developed an IGA procedure based on Reddy's HSDT to analyze the forced vibration of sandwich plates with an auxetic honeycomb core and laminated three-phase skin layers supported by KF under pulse loads. Investigation of the influence of some geometrical parameters and material properties on forced vibration of sandwich plates. From the results obtained, some main conclusions can be drawn as follows:

- ✓ The increase of λ_1 and θ has little effect on the displacement and stress response of the sandwich plate but has the effect of making the oscillations damp faster.
- ✓ Thicker honeycomb core layers cause larger plate displacements. In addition, laminated three-phase skin layers help to increase the strength of sandwich plates and protect the honeycomb core subjected to impulse loads, especially blast loads.
- ✓ The damping ratio helps the energy dissipation of the pulse load, and the vibration amplitude will decrease and achieve stability faster.
- ✓ The Kerr foundation helps reduce the displacement and stress response of the sandwich plate.

REFERENCES

[1]. Wan, H., Ohtaki, H., Kotosaka, S., & Hu, G. *"A study of negative Poisson's ratios in auxetic honeycombs based on a large deflection model"*. European Journal of Mechanics-A/Solids, 23(1), 95-106, (2004). DOI: https://doi.org/10.1016/j.euromechsol.2003.10.006

[2]. Zhang, X.-C., An, L.-Q., Ding, H.-M., Zhu, X.-Y., & El-Rich, M. *"The influence of cell micro-structure on the in-plane dynamic crushing of honeycombs with negative Poisson's ratio"*. Journal of Sandwich Structures & Materials, 17(1), 26-55, (2015). DOI: https://doi.org/10.1177/1099636214554180

[3]. Zhu, X., Zhang, J., Zhang, W., & Chen, J. *"Vibration frequencies and energies of an auxetic honeycomb sandwich plate"*. Mechanics of Advanced Materials and Structures, 26(23), 1951-1957, (2019).

[4]. Cong, P. H., Khanh, N. D., Khoa, N. D., & Duc, N. D. *"New approach to investigate nonlinear dynamic response of sandwich auxetic double curves shallow shells using TSDT"*. Composite Structures, 185, 455-465, (2018). DOI: https://doi.org/10.1016/j.compstruct.2017.11.047

[5]. Nguyen, D. D., & Pham, C. H. *"Nonlinear dynamic response and vibration of sandwich composite plates with negative Poisson's ratio in auxetic honeycombs"*. Journal of Sandwich Structures & Materials, 20(6), 692-717, (2018). DOI: https://doi.org/10.1177/1099636216674729

[6]. Pham, Q.-H., Nguyen, P.-C., Tran, T. T., & Nguyen-Thoi, T. *"Free vibration analysis of nanoplates with auxetic honeycomb core using a new third-order finite element method and nonlocal elasticity theory"*. Engineering with Computers, 1-19, (2023). https://doi.org/10.1007/s00366-021-01531-3

[7]. Cheng, Y., Zhang, K., Liang, B., Cheng, H., Hou, G., Xu, G., & Jin, W. *"Micromechanics of CNT grafted FRP based on hierarchical homogenization of transversely isotropic multi-coated model"*. International Journal of Mechanical Sciences, 161, 105014, (2019). DOI: https://doi.org/10.1016/j.ijmecsci.2019.105014

[8]. Swain, A., & Roy, T. *"Viscoelastic modelling and dynamic characteristics of CNTs-CFRP-2DWF composite shell structures"*. Composites Part B: Engineering, 141, 100-122, (2018).

[9]. Seidi, J., & Kamarian, S. *"Free vibrations of non-uniform CNT/fiber/polymer nanocomposite beams"*. Curved and Layered Structures, 4(1), 21-30, (2017). DOI: https://doi.org/10.1515/cls-2017-0003

[10]. Yousefi, Amir Hossein, et al. *"Dynamic characteristics of truncated conical panels made of FRPs reinforced with agglomerated CNTs."* Structures. Vol. 33. Elsevier, (2021). DOI: https://doi.org/10.1016/j.istruc.2021.07.046

[11]. Noroozi, Mohammad, Zajkani, Asghar, & Ghadiri, Majid. *"Dynamic plastic impact behavior of CNTs/fiber/polymer multiscale laminated composite doubly curved shells"*. International Journal of Mechanical Sciences, 195, 106223, (2021). DOI: https://doi.org/10.1016/j.ijmecsci.2020.106223

[12]. Hughes, Thomas JR, Cottrell, John A, & Bazilevs, Yuri. *"Isogeometric analysis: CAD, finite elements, NURBS, exact geometry and mesh refinement"*. Computer methods in applied mechanics and engineering, 194 (39-41), 4135-4195, (2005). DOI: https://doi.org/10.1016/j.cma.2004.10.008

[13]. Affdl, JC Halpin, & Kardos, JL. *"The Halpin-Tsai equations: a review"*. Polymer Engineering & Science, 16 (5), 344-352, (1976). DOI: https://doi.org/10.1002/pen.760160512
[14]. Nasution, Mahyuddin KM, Syah, Rahmad, Ramdan, Dadan, Afshari, Hassan, Amirabadi, Hossein, Selim, Mahmoud M,… Su, Chia-Hung. *"Modeling and computational simulation for supersonic flutter prediction of polymer/GNP/fiber laminated composite joined conical-conical shells"*. Arabian Journal of Chemistry, 15 (1), 103460, (2022). DOI: https://doi.org/10.1016/j.arabjc.2021.103460
[15]. Keshtegar, Behrooz, Motezaker, Mohsen, Kolahchi, Reza, & Trung, Nguyen-Thoi. *"Wave propagation and vibration responses in porous smart nanocomposite sandwich beam resting on Kerr foundation considering structural damping"*. Thin-Walled Structures, 154, 106820, (2020). DOI: https://doi.org/10.1016/j.tws.2020.106820
[16]. Reddy, Junuthula Narasimha. *"Mechanics of laminated composite plates and shells: theory and analysis"*: CRC press, (2003). DOI: https://doi.org/10.1201/b12409
[17]. Wolf J. *"Dynamic SoilStructure Interaction"*. PrenticeHall. Inc., Englewood Cliffs, New Jersey. (1985).
[18]. Abuteir, BW, Harkati, E, Boutagouga, D, Mamouri, S, & Djeghaba, K. *"Thermo-mechanical nonlinear transient dynamic and Dynamic-Buckling analysis of functionally graded material shell structures using an implicit conservative/decaying time integration scheme"*. Mechanics of Advanced Materials and Structures, 29(27), 5773-5792, (2022). DOI: https://doi.org/10.1080/15376494.2021.1964115

TÓM TẮT

Phân tích dao động cưỡng bức của tấm sandwich với lõi honeycomb và lớp da composite ba pha trên nền đàn hồi Kerr

Bài báo này giới thiệu phương pháp phân tích đẳng hình học (IGA) dựa trên lý thuyết biến dạng cắt bậc cao (HSDT) để phân tích dao động cưỡng bức của tấm sandwich đặt trên nền đàn hồi Kerr. Các tấm sandwich bao gồm một lớp lõi tổ ong siêu nhẹ và được gia cố bằng hai lớp da composite ba pha. Phương trình dạng yếu được suy ra từ nguyên lý Hamilton. Phương pháp Newmark-β được áp dụng để giải phương trình vi phân của tấm sandwich bằng chương trình được lập trong phần mềm Matlab. Độ chính xác của phương pháp đề xuất được xác minh thông qua các ví dụ so sánh. Sau đó, ảnh hưởng của kích thước hình học và tính chất vật liệu đối với dao động cưỡng bức của các tấm sandwich được nghiên cứu chi tiết.

Từ khoá: Tấm sandwich; Phân tích đẳng hình học; Auxetic honeycomb; Kerr foundation; Dao động cưỡng bức.